nature metabolism

ARTICLES

https://doi.org/10.1038/s42255-020-0178-9

Type 2 diabetes influences bacterial tissue compartmentalisation in human obesity

Fernando F. Anhê[1,2,5], Benjamin Anderschou Holbech Jensen[1,3,5], Thibault V. Varin[1], Florence Servant[4], Sebastian Van Blerk[4], Denis Richard[1], Simon Marceau[1], Michael Surette[2], Laurent Biertho[1], Benjamin Lelouvier[4], Jonathan D. Schertzer[2], André Tchernof[1] and André Marette[1]✉

Visceral obesity is a key risk factor for type 2 diabetes (T2D). Whereas gut dysbiosis appears to be instrumental for this relationship, whether gut-associated signatures translocate to extra-intestinal tissues and how this affects host metabolism remain elusive. Here we provide a comparative analysis of the microbial profile found in plasma, liver and in three distinct adipose tissues of individuals with morbid obesity. We explored how these tissue microbial signatures vary between individuals with normoglycaemia and those with T2D that were matched for body mass index. We identified tissue-specific signatures with higher bacterial load in the liver and omental adipose tissue. Gut commensals, but also environmental bacteria, showed tissue- and T2D-specific compartmentalisation. T2D signatures were most evident in mesenteric adipose tissue, in which individuals with diabetes displayed reduced bacterial diversity concomitant with fewer Gram-positive bacteria, such as *Faecalibacterium*, as opposed to enhanced levels of typically opportunistic Gram-negative Enterobacteriaceae. Plasma samples of individuals with diabetes were similarly enriched in Enterobacteriaceae, including the pathobiont *Escherichia–Shigella*. Our work provides evidence for the presence of selective plasma and tissue microbial signatures in individuals with severe obesity and identifies new potential microbial targets and biomarkers of T2D.

T2D is highly prevalent and has an increasing incidence worldwide, which compromises life and health span and exerts enormous pressure on health systems[1,2]. Visceral obesity is a major risk factor for T2D as well as for impaired glycaemic control (that is, glucose intolerance or prediabetes) that precedes overt T2D[2,3]. Prediabetes is characterised by high blood insulin, low-grade inflammation, insulin resistance, and elevated fasting or postprandial blood glucose. The latter increases the risk of all-cause mortality[2,3]. However, the key driving elements that connect visceral fat accumulation to prediabetes and overt T2D are ill-defined.

The gut microbiota is recognised as a major environmental determinant of obesity and T2D, and gut dysbiosis plays a central role in the development of chronic low-grade inflammation and in the pathogenesis of insulin resistance[4–8]. Gut bacteria and their fragments have been shown to translocate beyond the intestinal barrier, colonise and/or accumulate in the blood and extra-intestinal tissues[9,10], and trigger immunogenic pathways that can affect glucose homeostasis and other cardiometabolic outcomes[11–13]. Bacterial cell wall components, such as peptidoglycans and lipopolysaccharides (LPS), have been shown to alter immune and glucose homeostasis in both detrimental[14–16] and beneficial[17–19] ways, which suggests that bacterial translocation exerts a complex modulatory role in host metabolism. The way in which different body compartments accumulate bacterial fragments, or allow selective bacterial colonisation, remains elusive. An understanding of microbial signatures of obesity or T2D may reveal mechanisms of the chronic and compartmentalised inflammation that occurs during these diseases.

Although blood and tissue microbial profiles have been reported[9,10], their inter-organ signatures and relationship with prediabetes, glucose intolerance and T2D remain to be determined. In the present study we provide a comparative and contamination-aware analysis of the microbial profile found in plasma, liver and in three different adipose tissue depots (that is, omental, mesenteric and subcutaneous) of individuals with obesity. We determined the tissue microbial profiles in participants who are obese and normoglycaemic or obese and type 2 diabetetic. We found that T2D status dictated an extra-intestinal microbial signature, independent of obesity.

Results

Bacterial DNA abundance varies across different tissues in obese individuals. Biopsy samples from liver, mesenteric adipose tissue (MAT), omental adipose tissue (OAT), subcutaneous adiopse tissue (SAT) and plasma samples were collected from individuals with severe obesity during bariatric surgery procedures. Samples were processed along with a comprehensive set of negative controls and were used for 16S ribosomal RNA-based bacterial quantification and taxonomic profiling (Fig. 1). Participants were 42 ± 9 years old and their average body mass index (BMI) was 50.5 kg m^{-2} (Table 1). Several patients presented some degree of liver steatosis ($34.4\% \pm 28.1\%$ steatosis) and dyslipidaemia, as revealed by circulating triglyceride levels (1.9 ± 0.75 mmol l^{-1}) as well as total lipoprotein (4.5 ± 0.8 mmol l^{-1}), high-density lipoprotein (HDL) (1.2 ± 0.3 mmol l^{-1}), and low-density lipoprotein (LDL) (2.5 ± 0.8 mmol l^{-1}) cholesterol levels (Table 1). Mean fasting

[1]Québec Heart and Lung Research Institute, Laval University, Québec, Québec, Canada. [2]Department of Biochemistry and Biomedical Sciences, Farncombe Family Digestive Health Research Institute and Centre for Metabolism Obesity and Diabetes Research, McMaster University, Hamilton, Ontario, Canada. [3]Novo Nordisk Foundation Center for Basic Metabolic Research, Faculty of Health and Medical Sciences, University of Copenhagen, Copenhagen, Denmark. [4]Vaiomer, Labège, France. [5]These authors contributed equally: Fernando F. Anhê, Benjamin Anderschou Holbech Jensen. ✉e-mail: andre.marette@criucpq.ulaval.ca

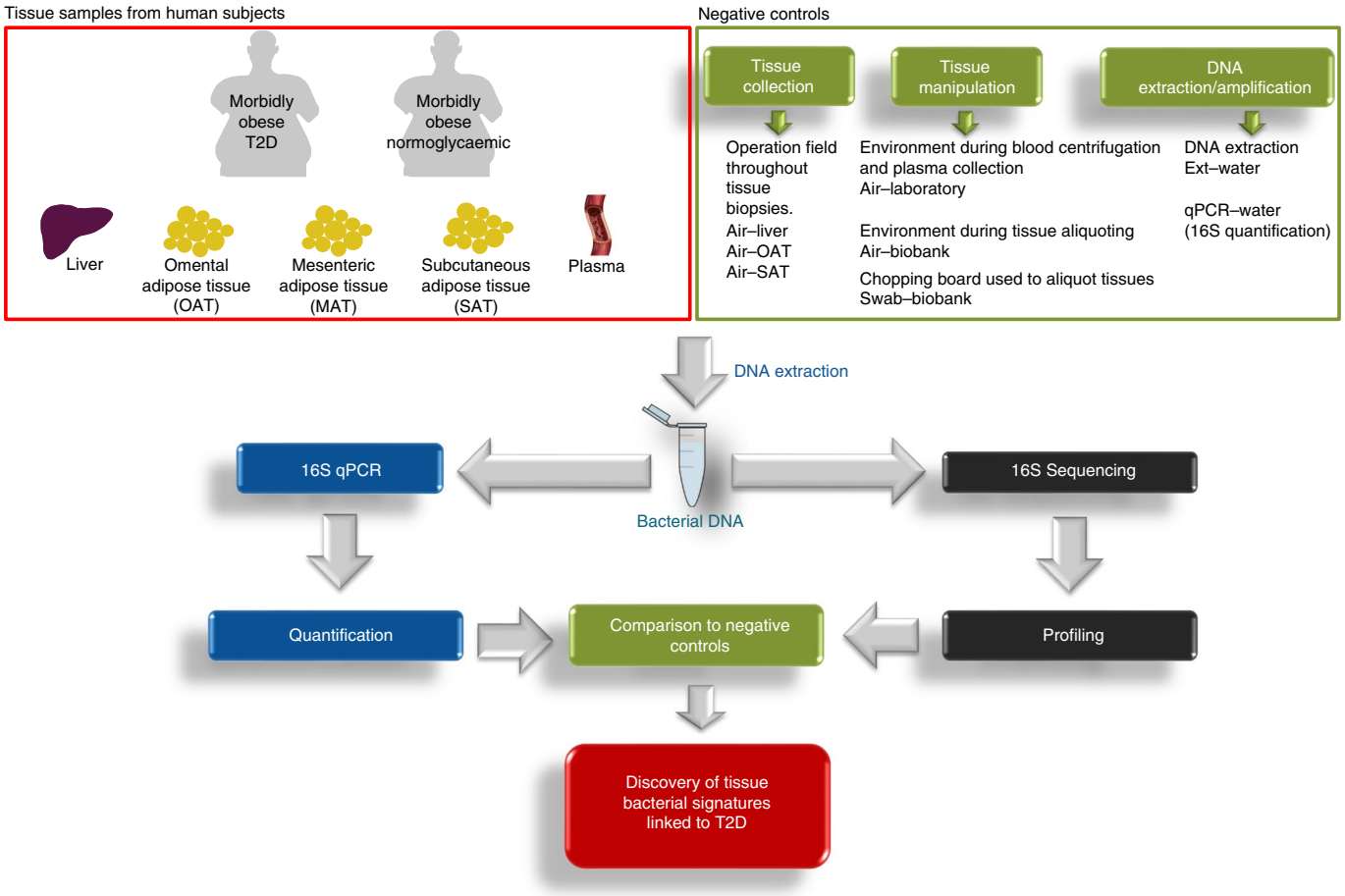

Fig. 1 | Workflow overview. Liver, three different adipose tissue depots (OAT, MAT and SAT) and plasma samples were collected from individuals with morbid obesity who had T2D ($n=20$) and from those who had normoglycaemia ($n=20$). DNA extraction and amplification procedures were carried out using optimised conditions for bacterial DNA detection in blood plasma and tissues. A comprehensive set of negative controls was tested to control for environmental sample contamination at major steps in the analysis: tissue collection, tissue manipulation, and DNA extraction and amplification. During tissue collection, tubes were kept open next to the operation field throughout the entire procedure (air-liver, air-OAT, and air-SAT). Contamination coming from tissue manipulation was controlled by another set of tubes that were kept open next to the operator throughout blood centrifugation and plasma collection (air-laboratory) as well as during tissue aliquoting (air-biobank). The chopping board used to aliquot tissues was sampled prior to tissue manipulation (swab-biobank). Water samples were used to control for labware, reagent and/or environmental contamination during DNA extraction (ext-water) and amplification steps for tissue 16S rRNA quantification by quantitative PCR (qPCR-water). After thorough validation of negative controls on a case-by-case basis, 16S quantification and sequencing data were used in the discovery of tissue-specific bacterial signatures linked to T2D.

blood glucose and glycated haemoglobin (HbA1c) levels were 8.1 ± 3.7 mmol l^{-1} and 6.8 ± 1.6 %, respectively. Stratification according to diabetic status is presented in Table 1.

We found a similar number of 16S rRNA gene copies in both MAT and SAT. Conversely, 16S rRNA was found to be considerably more abundant in the liver than in any other tissue, except for OAT (Fig. 2a). The 16S rRNA gene count was approximately 1,000-fold higher in tissue samples than in negative controls, which suggests that sample contamination would have been of low impact in these determinations. In plasma samples, however, the 16S rRNA gene count was closer to that which was found in negative controls (Fig. 2a). Lower 16S rRNA gene counts in plasma, as compared to whole blood and buffy coat samples, have been reported previously[9]. Our findings should therefore be interpreted with caution, and qualitative assessment of 16S rRNA sequences in plasma should be validated against negative controls on a case-by-case basis[20,21]. Overall, these data suggest tissue-specific bacterial compartmentalisation with preferential deposition of bacterial fragments and/or bacterial colonisation in the liver and OAT, two major organs involved in metabolic control.

Metabolic tissues display specific bacterial DNA signatures. We next assessed, by 16S rRNA gene-based sequencing, bacterial profiles in the plasma, hepatic, and adipose tissues of participants with obesity. Higher number of operational taxonomic units (OTUs) were found in the MAT as compared to liver and plasma (Fig. 2b). These differences, however, were lost when alpha diversity accounted for evenness (Fig. 2c).

To assess overall tissue-specific clustering of 16S rRNA sequences (beta diversity), we calculated generalised UniFrac distances, identified the dimensions that better explained variance and plotted on principal coordinate analysis (PCoA) scatterplots. A small, yet significant, tissue-specific clustering was displayed by 16S rRNA sequences and 14% of the variation was explained by PCoA1, which mainly accounted for the differences between MAT and the other tissues; tissue-specific clustering among liver, OAT, SAT and plasma explained 6.5% of the observed variation (Fig. 2d).

Analysis at phylum level revealed a dominance of Proteobacteria in the five tissues under study, followed by Firmicutes, Actinobacteria and Bacteroidetes (Fig. 2e). The MAT exhibited a more distinct bacterial profile at phylum level, marked by a higher presence of

Table 1 | Sample characteristics

	Cohort		Non-diabetic		Diabetic			
	Mean	s.d.	Mean	s.d.	Mean	s.d.	*P* value	*q* value
Sample size	40		20		20			
Men	10		5		5			
Women	30		15		15			
Age	42	9	41	9	42	9	0.5418[a]	0.90189
Weight (kg)	140	26	139	24	141	29	0.8403[a]	0.90899
Height (cm)	166	8	166	7	166	9	0.9680[a]	0.90899
BMI	50.5	8.4	50.2	7.9	50.9	9.1	0.8150[b]	0.90899
Waist circumference (cm)	139.6	14.5	136.5	12.6	142.8	15.8	0.1695[a]	0.51359
Hip circumference (cm)	148.4	15.6	149.6	15.2	147.2	16.2	0.4731[b]	0.90189
Waist–hip ratio	0.9	0.1	0.92	0.09	0.97	0.07	0.0504[a]	0.22907
Steatosis (%)	34.4	28.1	34.0	29.4	34.8	27.5	0.9307[b]	0.90899
Steatosis grade	1.5	0.9	1.5	0.9	1.5	0.9	0.9158[b]	0.90899
HbA1c (%)	6.8	1.6	5.5	0.4	8.1	1.2	<0.0001[b]	0.00091
Fasting glucose (mmol l^{-1})	8.1	3.7	5.3	0.5	10.9	3.5	<0.0001[b]	0.00091
Total cholesterol (mmol l^{-1})	4.5	0.8	4.7	0.8	4.3	0.8	0.0893[a]	0.32469
HDL cholesterol (mmol l^{-1})	1.2	0.3	1.2	0.2	1.1	0.3	0.6140[a]	0.90899
LDL cholesterol (mmol l^{-1})	2.5	0.8	2.8	0.7	2.2	0.7	0.0160[a]	0.09696
Triglycerides (mmol l^{-1})	1.9	0.9	1.7	0.7	2.1	1.1	0.3870[b]	0.87946
Total_chol to HDL_chol ratio	4.1	1.2	4.3	1.4	3.9	0.9	0.5457[b]	0.90189
AST (U l^{-1})	35.1	21.9	36.5	25.6	33.7	17.9	0.6585[b]	0.90899
ALT (U l^{-1})	27.1	13.0	27.8	12.7	26.4	13.9	0.8622[b]	0.90899
NASH	1.4	1.0	1.4	1.0	1.4	0.9	>0.9999[b]	0.90899
Fibrosis	0.8	0.9	0.6	0.6	1.0	1.0	0.2968[b]	0.77083

[a]Unpaired two-sided *t*-test, for comparisons that passed Shapiro–Wilk normality test [b]Mann–Whitney two-sided *U* test, for comparisons that did not pass the Shapiro–Wilk normality test Two-stage linear step-up procedure of Benjamini, Krieger and Yekutieli, with $q < 1\%$. $n = 20$ per group, except for alanine aminotransaminase (ALT) and aspartate aminotransaminase (AST) for which diabetic, $n = 12$ and non-diabetic, $n = 13$. NASH, nonalcoholic steatohepatitis.

Bacteroidetes as compared to liver and SAT. This phylum also trended higher in the MAT versus OAT and MAT versus plasma comparisons (Fig. 2e). The MAT displayed a tendency towards lower relative abundance of Proteobacteria and significantly lower relative abundance of Actinobacteria when compared to the liver. Overall, these results indicate the presence of tissue-specific bacterial compartmentalisation with more pronounced differences in taxonomy found in the MAT.

To identify tissue-specific bacterial signatures at genus level, we first filtered all taxa that were not present in at least 20% of samples within each tissue and found 84 genera distributed across the five body sites under investigation (Extended Data Fig. 1). We next used the ALDEx2 software package to extract the genera with higher likelihood to constitute tissue-specific signatures and tested their specificity using a Kruskal–Wallis test with Dunn's pairwise comparison followed by Bonferroni–Holm adjustment. Because no qualitative differences were observed among all groups of negative controls (Fig. 2b,c and Extended Data Fig. 2) we condensed them into a single group in the subsequent analyses.

Pseudomonas was the predominant genus that was found across all tissues. This group includes soil and water bacteria as well as potential human pathogens. We found a significantly higher relative abundance of *Pseudomonas* in tissues as compared to plasma and negative controls, but not between the latter two samples (Fig. 3a). Furthermore, we observed a preferential compartmentalisation of *Arthrobacter* and *Ruminococcus* in the liver (Fig. 3b,c). *Arthrobacter* is a genus of bacteria that is normally found in soil and water, whereas *Ruminococcus* is a known member of the human gut microbiota. Levels of *Arthrobacter* and *Ruminococcus* in negative control samples were significantly lower than those in liver samples, which indicates a low incidence of environmental sample contamination.

Eight genera showed preferential compartmentalisation in adipose tissues. *Bacteroides* showed a pronounced preference to MAT depots (Fig. 3d), whereas *Faecalibacterium* displayed a higher proportion in the MAT versus SAT and MAT versus plasma, but not in the MAT versus liver and MAT versus OAT comparisons (Fig. 3e). Furthermore, *Enterobacter* showed higher deposition in the OAT and SAT (Fig. 3f). *Bacteroides, Faecalibacterium* and *Enterobacter* are probably dispersed from the gut microbiota, whereas OAT and SAT also showed higher presence of the following groups of environmental bacteria: *Burkholderia*, *Corynebacterium* and *Kluyvera* (Fig. 3g–i). Moreover, the environmental bacterial genus *Paracoccus* showed a preferential distribution in the SAT (Fig. 3j), whereas *Acinetobacter*, another soil and water inhabitant, showed a similar distribution in all adipose tissues (Fig. 3k). All taxa with preferential compartmentalisation in adipose tissues displayed significantly higher relative abundance in tissue samples than in negative control samples, which corroborates the indication of low interference from sample contamination (Fig. 3d–k). This is also supported by at least a 1,000-fold increase in 16S rRNA gene copy number between tissues and negative controls (Fig. 2a).

We identified several genera with specific compartmentalisation in plasma. Of these, *Rhodoferax* and *Polaromonas* were the only genera that were statistically more abundant in plasma than in negative control samples (Fig. 3l,m). *Legionella*, *Escherichia–Shigella*, *Flavobacterium*, *Mucilaginibacter*, and *Pedobacter* all

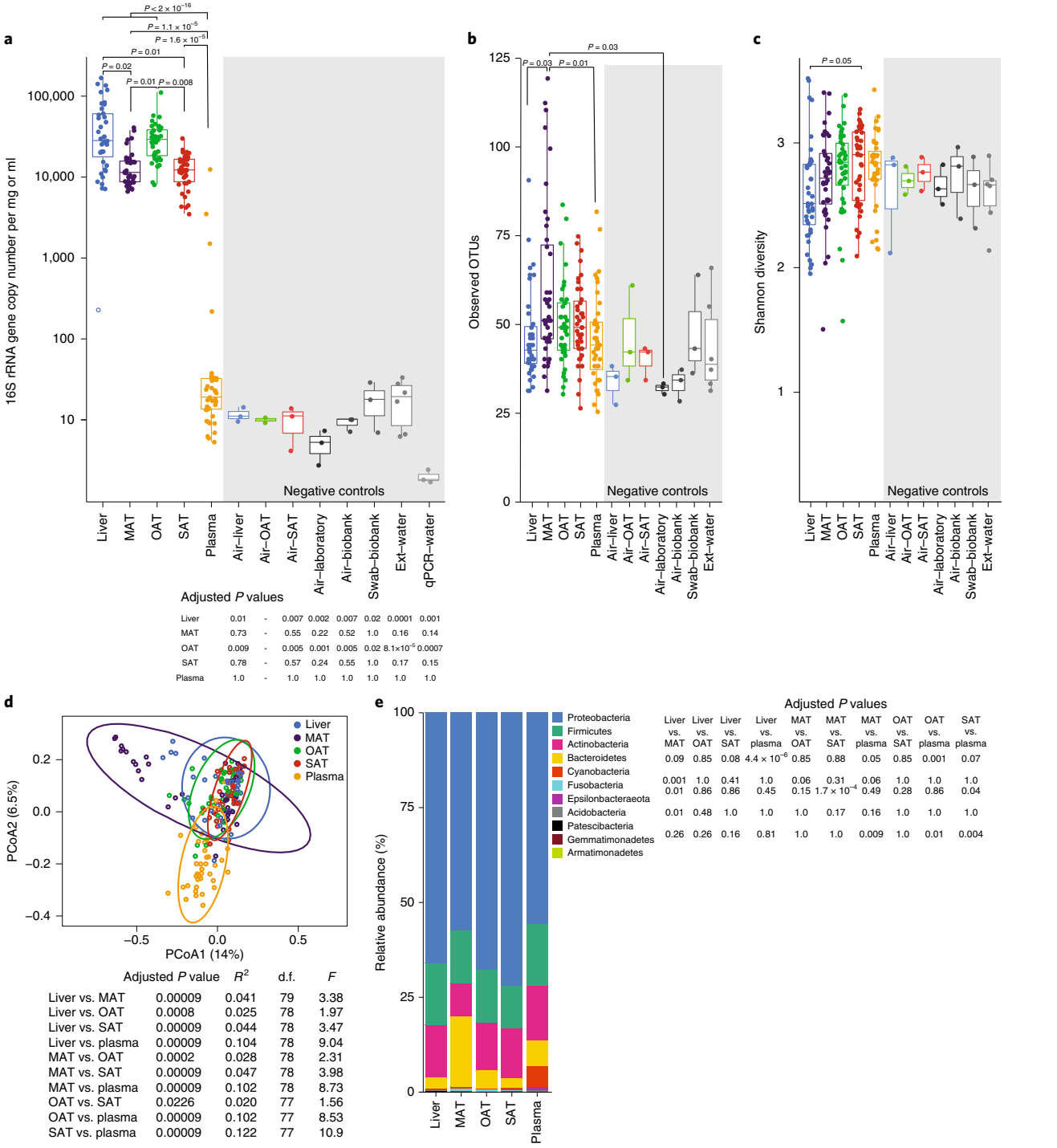

Adjusted *P* values	Liver vs. MAT	Liver vs. OAT	Liver vs. SAT	Liver vs. plasma	MAT vs. OAT	MAT vs. SAT	MAT vs. plasma	OAT vs. SAT	OAT vs. plasma	SAT vs. plasma
Bacteroidetes	0.09	0.85	0.08	4.4×10^{-6}	0.85	0.88	0.05	0.85	0.001	0.07
Cyanobacteria	0.001	1.0	0.41	1.0	0.06	0.31	0.06	1.0	1.0	1.0
Fusobacteria	0.01	0.86	0.86	0.45	0.15	1.7×10^{-4}	0.49	0.28	0.86	0.04
Epsilonbacteraeota	0.01	0.48	1.0	1.0	1.0	0.17	0.16	1.0	1.0	1.0
Acidobacteria	0.26	0.26	0.16	0.81	1.0	1.0	0.009	1.0	0.01	0.004

Adjusted *P* value	R^2	d.f.	*F*
Liver vs. MAT	0.00009	0.041	79	3.38
Liver vs. OAT	0.0008	0.025	78	1.97
Liver vs. SAT	0.00009	0.044	78	3.47
Liver vs. plasma	0.00009	0.104	78	9.04
MAT vs. OAT	0.0002	0.028	78	2.31
MAT vs. SAT	0.00009	0.047	78	3.98
MAT vs. plasma	0.00009	0.102	78	8.73
OAT vs. SAT	0.0226	0.020	77	1.56
OAT vs. plasma	0.00009	0.102	77	8.53
SAT vs. plasma	0.00009	0.122	77	10.9

Fig. 2 | Bacterial distribution across body sites. a, 16S rRNA gene counts. **b**, Observed OTUs. **c**, Shannon index in the liver, three different adipose tissue depots (OAT, MAT and SAT) and plasma of participants with obesity. Negative controls were tested to control for environmental sample contamination at major steps in the analysis: tissue collection (air-liver, air-OAT, air-SAT), tissue manipulation (air-laboratory, air-biobank and swab-biobank) and DNA extraction or amplification (ext-water, qPCR-water). In panels **a**–**c** and **e**, groups were compared using a Kruskal–Wallis one-way ANOVA followed by Dunn's test for pairwise comparison and *P* value adjustment using the Bonferroni–Holm method. Box plots depict the first and the third quartile with the median represented by a vertical line within the box; the whiskers extend from the first and third quartiles to the highest and lowest observation, respectively, not exceeding 1.5×IQR. **d**, PCoA on generalised UniFrac distances. PERMANOVA, with subsequent Bonferroni–Holm *P* value adjustment, was used to assign statistical significance to the differences between clusters of 16S rRNA sequences. **e**, Phylum distribution in different tissues: Bonferroni–Holm adjusted *P* values are shown only for phyla that passed the analysis of variance (Kruskal–Wallis) test. The numbers of independent biological samples analysed in panel **a** were: liver ($n=39$), MAT ($n=40$), OAT ($n=40$), SAT ($n=40$), plasma ($n=39$), air-liver ($n=3$), air-OAT ($n=2$) and air-SAT ($n=3$), and in panels **b** and **c** were: liver ($n=40$), MAT ($n=40$), OAT ($n=39$), SAT ($n=39$), plasma ($n=39$), air-liver ($n=3$), air-OAT ($n=2$) and air-SAT ($n=3$). In panels **d** and **e** the numbers of independent biological replicates tested were: liver ($n=40$), MAT ($n=40$), OAT ($n=39$), SAT ($n=39$) and plasma ($n=39$).The numbers of technical replicates tested in panels **a**–**c** were: air-laboratory ($n=3$), air-biobank ($n=3$), swab-biobank ($n=3$), ext-water ($n=6$) and qPCR-water ($n=3$). Each circle represents a sample. All statistical tests were two-sided, and differences were considered to be statistically significant at $P<0.05$.

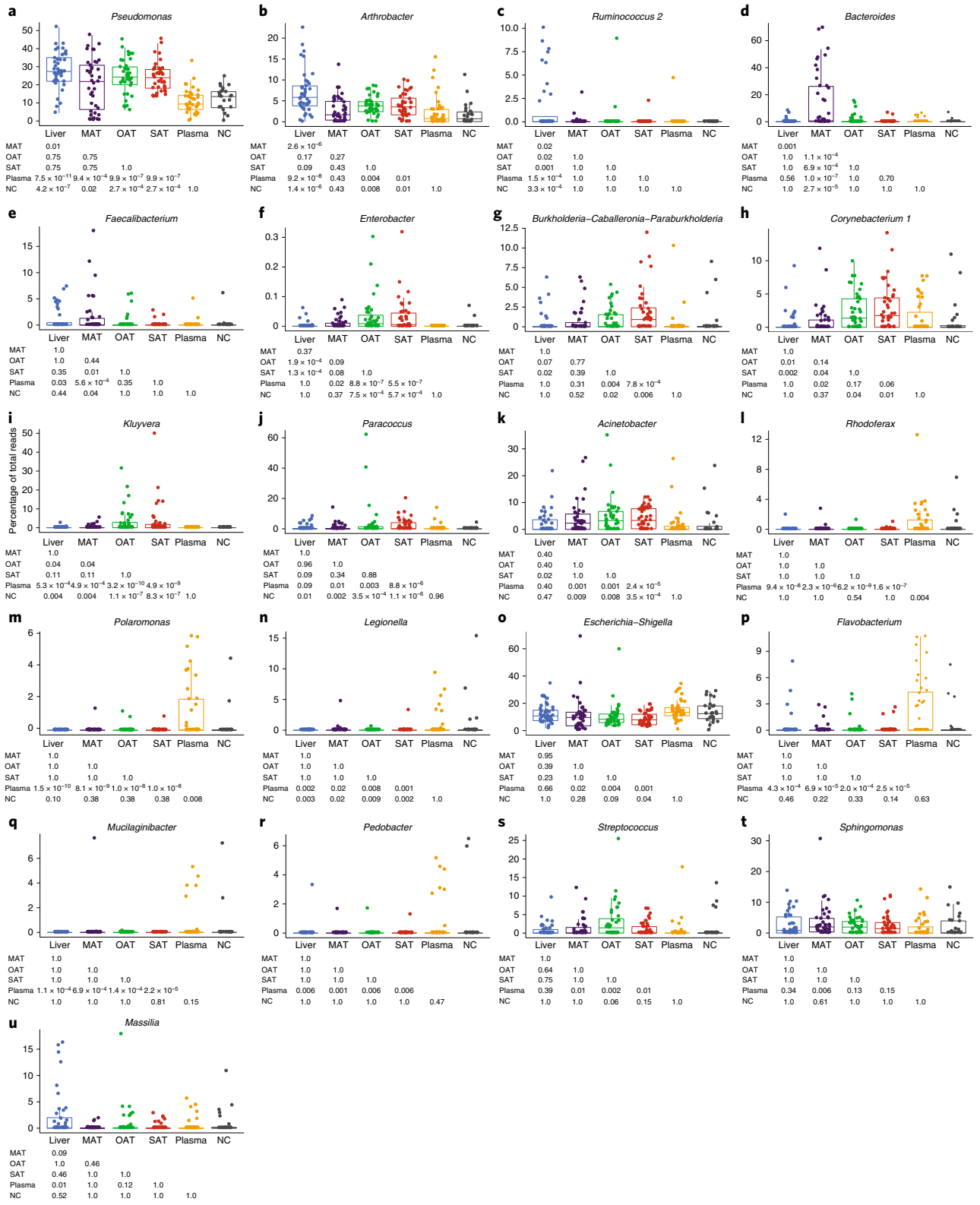

Fig. 3 | Tissue-specific bacterial signatures. Taxa that were not present in at least 20% of samples within each tissue were removed from analysis. ALDEx2 was used to extract the genera with higher likelihood to constitute tissue-specific signatures. **a**–**u**, The relative abundance of each genus was then compared between different tissue depots (liver, OAT, MAT, SAT and plasma) of obese individuals and negative controls (NC) by using a Kruskal–Wallis test with Dunn's pairwise comparison followed by Bonferroni–Holm adjustment. Box plots depict the first and the third quartile of relative abundances with the median represented by a vertical line within the box; the whiskers extend from the first and third quartiles to the highest and lowest observation, respectively, not exceeding 1.5 × IQR. The numbers of independent biological replicates tested were: liver ($n = 39$), MAT ($n = 40$), OAT ($n = 40$), SAT ($n = 40$), plasma ($n = 39$) and NC ($n = 23$). Adjusted P values for pairwise comparison are shown below each plot. Each circle represents a sample. All statistical tests were two-sided, and differences were considered to be statistically significant at $P < 0.05$.

showed relative abundance in plasma comparable to that in negative controls (Fig. 3n–r), which suggests that signatures that are found in plasma should be taken with more caution than those obtained from tissues. We observed some degree of variation in the presence of *Streptococcus*, *Sphingomonas*, and *Massilia* across body sites. However, pairwise comparisons did not indicate significant tissue-specificity for these taxa (Fig. 3s–u).

Tissue-specific taxa differ between individuals with and without type 2 diabetes independently of obesity. Individuals were subsequently assigned to groups according to their fasting blood glucose values. The anthropometric and metabolic parameters of individuals with T2D and individuals without diabetes (non-diabetic, ND) are presented in Table 1. No differences in body features and markers of dyslipidaemia were found among groups, whereas individuals with T2D presented significantly higher fasting blood glucose and glycated haemoglobin levels as compared to individuals without diabetes (Table 1).

No differences in 16S rRNA gene counts were found within each tissue when comparing participants with T2D versus participants without diabetes (Fig. 4a). However, we identified a numerical increase in observed OTUs in the MAT of individuals without diabetes versus that of patients with T2D (Fig. 4b), which became significant when evenness was considered (by means of the Shannon diversity index), and which supports the existence of a more evenly distributed microbiota in the MAT of individuals without diabetes than in patients with T2D (Fig. 4c). These data point towards bacterial diversity in the MAT being linked to better blood glucose control, which might mirror higher bacterial diversity in the gut microbiota of individuals without diabetes, as has been reported previously[22].

We next analysed beta diversity across different body sites of patients with T2D versus individuals without diabetes. PCoA analysis on generalised UniFrac distances revealed no diabetes state-driven clustering across different tissues (Fig. 4d–h). We applied linear discriminant analysis effect size (LEfSe) to explore the taxa that better discriminated bacterial populations within each body site and between disease states. Most taxa that were shown to significantly discriminate between patients with T2D and individuals without diabetes were found in the MAT (Fig. 4j). Although the MAT of individuals with T2D showed higher levels of Enterobacteriaceae, it showed lower abundance of certain Firmicutes (that is, *Faecalibacterium* and *Romboutsia*), Bacteroidetes (that is, *Odoribacter* and *Alistipes*) and Deltaproteobacteria (that is, *Bilophila*) than did the MAT of individuals without diabetes (Fig. 4j). Our findings corroborate previous reports that link the family Enterobacteriaceae to poor glycaemic control[23,24] and *Faecalibacterium*[22,24,25], *Odoribacter*[26] and *Alistipes*[22,24,27] to leanness and positive metabolic outcomes, which suggests that these taxa can find a niche in the MAT to modulate glucose homeostasis in the host. *Bilophila* is a genus that contains bile acid-resistant bacteria that are generally linked to obesity[28]; however, its effect on blood glucose regulation without the confounding factor of obesity is largely unknown. Our data suggest that compartmentalisation of certain *Bilophila* species in the MAT may positively contribute to blood glucose control independently of obesity. Two families of water and soil bacteria, Marinifilaceae and Xanthobacteriaceae, were enriched in the MAT of individuals without diabetes (Fig. 4j), which suggests that environmental bacteria—and/or their fragments—that are present in food and water can accumulate in the MAT and may affect blood glucose regulation. This observation is well-aligned with a recent report that investigated the positive impact on gut immunity and host metabolism of a related environmental bacterium[29].

We identified some bacteria that are commonly found in water and soil and that have distinct distributions in the liver, OAT and SAT of patients with T2D and individuals without diabetes. *Aquabacterium* and Moraxellaceae were enriched in the liver of patients with T2D and individuals without diabetes, respectively (Fig. 4i). The OAT of individuals without diabetes showed higher levels of *Arthrobacter* and Burkholderiaceae (Fig. 4k). In the SAT, *Sphingomonas* were enriched in patients with T2D, whereas *Caulobacter* and bacteria of the family 67–14 were more abundant in samples from individuals without diabetes (Fig. 4l).

In the plasma of patients with T2D, we found a more pronounced deposition of two genera from the Enterobacteriaceae family—*Escherichia–Shigella* and *Serratia*—as well as a higher presence of Neisseriaceae than was found in individuals without diabetes (Fig. 4m). These findings are in line with higher levels of Enterobacteriaceae being a strong predictor of higher glycaemic load after a meal[23]. Furthermore, *Escherichia–Shigella* has been linked to insulin resistance[8] and has been shown to be the sole taxon that is enriched in patients with T2D when accounting for the confounding factors of obesity and glucose-lowering treatments[24]. Our findings add to this previous knowledge as they show that live and/or fragmented *Escherichia–Shigella*, as well as other Enterobacteriaceae, can access and build up in the circulatory compartment potentially affecting glucose homeostasis. Although these three taxa showed similar relative abundances in plasma and negative controls (Extended Data Fig. 3i), when factoring in 16S rRNA gene counts *Escherichia–Shigella*, *Serratia* as well as their family Enterobacteriaceae showed higher counts than were observed in negative controls ($P = 0.06$; Extended Data Fig. 3j). Although this suggests that sample contamination may have accounted for some 16S rRNA sequences having been annotated as *Escherichia–Shigella, Serratia* and potentially other Enterobacteriaceae, disease-specific signatures for these taxa that are identified in plasma strongly point to a credible biological phenomenon (Extended Data Fig. 3p–r).

Discussion

Bacterial translocation and tissue deposition are subjects of intense debate[20], with environmental and processing contamination known to constitute a potential confounding factor[30–32]. Here, we included extensive sets of controls at each tissue and sequencing manipulation step, from operating room to biobanking, exposure to laboratory air and 16S rRNA gene sequencing, followed by rigorous statistical testing to mitigate the risk of reporting false-positive results. We provide evidence of compartmentalised bacterial colonisation and/or fragment deposition in extra-intestinal tissues, with higher 16S rRNA gene counts found in the liver and OAT, as compared to those found in the MAT, SAT and plasma of individuals with morbid obesity. In addition, tissue-specific bacterial signatures revealed a more pronounced relative abundance of gut colonisers in the MAT. This profile is consistent with the anatomical route followed by bacteria through the gut–liver axis and with translocation of gut bacteria past the intestinal barrier to the neighbouring adipose tissue in the mesentery, which is extensively patrolled by gut-residing immune cells[33].

In agreement with previous reports, our results show that the relative abundance of taxa in the tissues is potentially confounded by sample contamination in a taxon-specific manner and should be analysed on a case-by-case basis[20]. It is important to stress that relative abundance does not account for the absolute quantity of taxa. This is particularly relevant when negative controls are compared to other tissues, as the latter showed approximately 1,000 times more copies of the 16S rRNA gene than the former (Fig. 2a). For this reason, sample contamination is potentially a more important issue for plasma samples in our data set. However, as shown by rigorous statistical tests, tissue-specific, as well as diabetes state-specific, bacterial deposition—even in plasma—is not random, and contamination would be unlikely to favour one tissue or disease state over

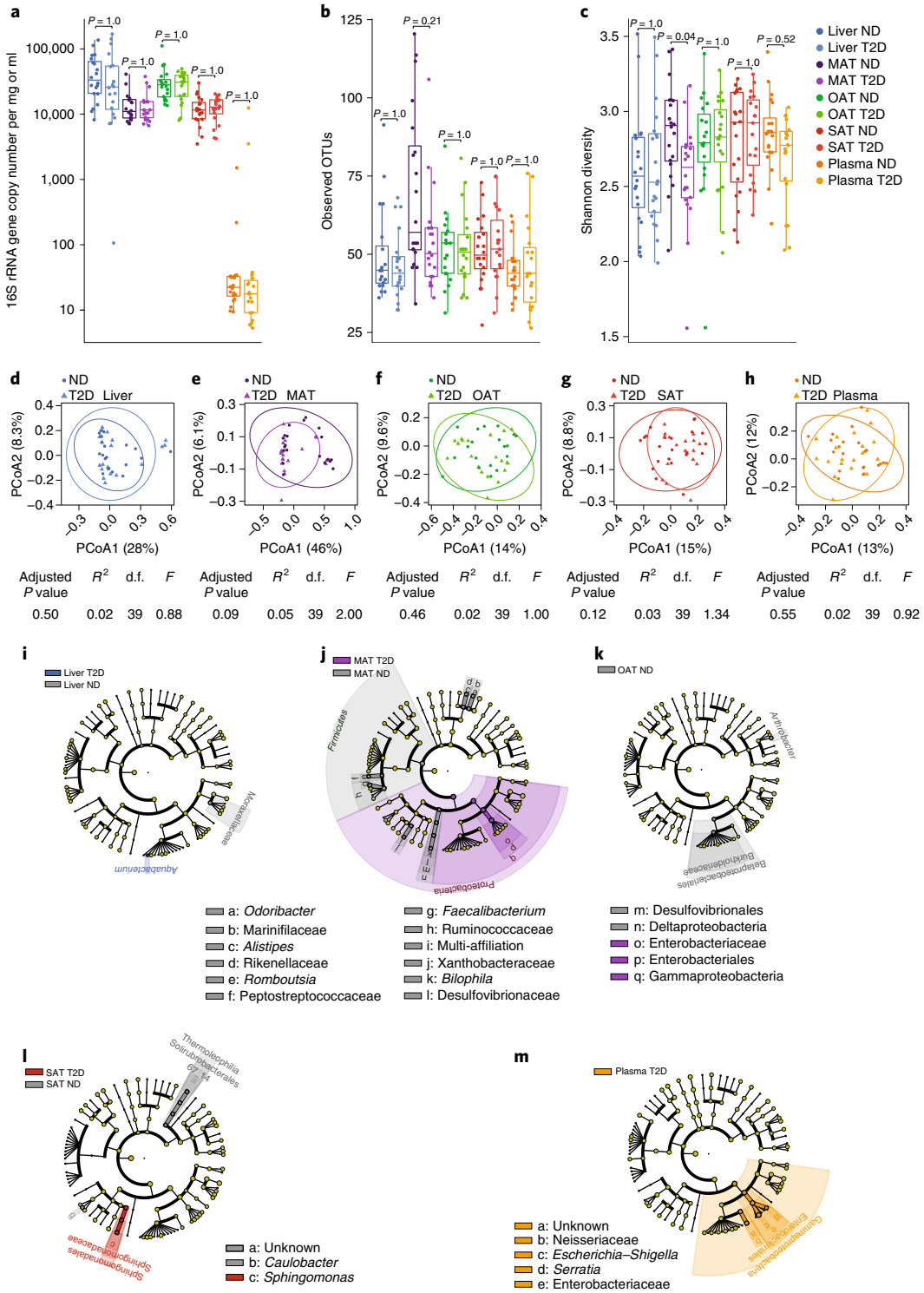

Fig. 4 | Tissue bacterial profile in participants with normoglycaemia or type 2 diabetes. a–c, 16S rRNA gene counts (**a**), observed OTUs (**b**) and Shannon index (**c**) within different tissues of patients with T2D and individuals without diabetes (ND). In panels **a**–**c**, groups were compared using a Kruskal–Wallis one-way ANOVA followed by Dunn's test for pairwise comparison and *P* value adjustment using the Bonferroni–Holm method. Box plots depict the first and the third quartile with the median represented by a vertical line within the box; the whiskers extend from the first and third quartiles to the highest and lowest observation, respectively, not exceeding 1.5 × IQR. **d**–**h**, PCoA on generalised UniFrac distances found within tissues and between disease states (T2D versus ND). PERMANOVA, with subsequent Bonferroni–Holm *P* value adjustment, was used to assign statistical significance to the differences between clusters of 16S rRNA sequences depicted in each panel. LEfSe effect size was used to calculate the taxa that better discriminated between disease states and within tissue, and these were plotted in cladograms (**i**–**m**). The numbers of independent biological replicates tested were: panel **a**, liver T2D ($n = 19$), liver ND ($n = 20$), MAT T2D ($n = 20$), MAT ND ($n = 20$), OAT T2D ($n = 20$), OAT ND ($n = 20$), SAT T2D ($n = 20$), SAT ND ($n = 20$), plasma T2D ($n = 19$) and plasma ND ($n = 20$); panels **b**–**m**, liver T2D ($n = 20$), liver ND ($n = 20$), MAT T2D ($n = 20$), MAT ND ($n = 20$), OAT T2D ($n = 19$), OAT ND ($n = 20$), SAT T2D ($n = 19$), SAT ND ($n = 20$), plasma T2D ($n = 19$) and plasma ND ($n = 20$). Each square, circle and triangle represents a sample. All statistical tests were two-sided, and differences were considered to be statistically significant at $P < 0.05$.

another. In fact, diabetes state-driven bacterial deposition in plasma was found to be significantly lower than that of negative controls when data were corrected by 16S rRNA gene load, which further supports the biological relevance of our findings. Furthermore, *Escherichia–Shigella* was shown to be enriched in the plasma of patients with diabetes, which is in agreement with several previous studies that reported higher levels of *Escherichia–Shigella* in the faeces of individuals with dysglycaemia[8,23,24].

Our results find support in previous studies that report bacterial colonisation in blood and tissues in healthy and disease states[9,10,12,13], and further suggest that environmental bacteria, which are likely to be present in food and water, may cross the gut barrier to accumulate in the blood and organs. Most environmental bacteria that are increasingly found to be present in patients with T2D can be linked to widespread nosocomial infections that are often distributed via hospital water supplies. Because patients with diabetes are usually more frequently hospitalised than their counterparts without diabetes, they are at greater risk of contracting infections and therefore may acquire part of their tissue microbiota during such visits. Hyperglycaemia decreases barrier function[34] and individuals with T2D may therefore represent a particularly vulnerable group who may be susceptible to translocation of ingested bacteria. We also reason that environmental bacteria may by-pass the immunological filter in the gut more easily than gut commensals, as the latter contribute to the maturation of immune responses in the host from early life. It is also possible that enteric immune cells that reside in the lamina propria may enable processed bacteria sampled from the lumen to initiate immune responses, which may also contribute to the entrance of bacteria (and/or their components) into the system and, which presumably, and more importantly, may affect bacterial deposition in the MAT. Altered immunity[35] and gut microbial dysbiosis are typical obesity-related traits that act in concert to produce compartmentalised responses that ultimately dictate metabolic outcomes in the host[36,37]. These findings support the hypothesis that environmental bacteria can reach specific niches at various body sites and potentially influence glycaemic control. However, we acknowledge that we cannot fully exclude the presence of spurious contamination from environmental taxa, especially in plasma samples, despite the rigorous methodological and statistical approaches used here. For this reason, more studies are warranted to confirm the biological relevance of these findings.

We cannot determine whether the identified 16S rRNA gene sequences came from live, senescent or fragmented bacteria. Schierwagen et al. were able to cultivate *Staphylococcus* and *Acinetobacter* (a group of environmental bacteria) using blood samples, which matched their findings by 16S rRNA gene sequencing and is in line with the numerous studies that identify living bacteria in the blood of healthy individuals by culture methods and microscopy[38]. However, given the chemical and mechanical stress that is inherent to digestion, and the fact that these patients did not display sepsis or any sign of bacterial infection, we speculate that the majority of the 16S rRNA sequences annotated in this study were from fragmented bacteria, which would facilitate translocation past the leaky gut barrier of participants with obesity.

In summary, we have provided contamination-aware evidence for distinct microbial signatures in multiple body sites of the same individual and found tissue- as well as T2D-specific bacterial compartmentalisation in individuals that are morbidly obese but are matched for BMI. Further studies are warranted to identify physiological traits that predispose to bacterial translocation and to investigate to what extent live bacteria or bacterial components that are found in metabolically relevant tissues promote or respond to T2D status. It would be of major interest to identify bacteria or bacterial components that preserve glucose regulation in individuals with both normoglycaemia and morbid obesity.

Methods

Participants. Tissue samples were obtained from the biobank of the Institut Universitaire de Cardiologie et de Pneumologie de Québec, Université Laval (IUCPQ) according to institutionally approved management procedures. Ethical approval was granted by the Canadian Institute of Health and Research, policy no. 2017-2746 21386. All participants provided written informed consent. Biological samples were harvested from a right flank trocar incision (SAT), greater omentum (OAT) and mesentery from transverse colon (MAT), in addition to blood and liver biopsies. All samples were harvested at the beginning of the surgery under aseptic conditions. Upon sampling, specimens were immediately flash frozen in the operating room and were subsequently stored at −80 °C. Patients received antibiotic prophylaxis at the time of anaesthesia induction (2 g of IV cefazolin for patients between 80 and 120 kg and 3 g for patients above 120 kg). The cohort included 10 men and 30 women, which reflects the proportion of each sex in the IUCPQ bariatric practice. A total of $n = 20$ participants (5 men and 15 women) had normal glucose tolerance described by a HbA1c below 5.7% or fasting plasma glucose below 6.1 mM, whereas $n = 20$ participants (5 men and 15 women) had T2D, with fasting plasma glucose above 7.0 mM or HbA1c ≥ 6.5 %. These groups were matched for key metabolic biometrics (Table 1).

Waist and hip circumferences were measured at the umbilical and upper thigh level, respectively. Cholesterol and triglyceride levels were measured using an automated enzymatic method in both plasma and HDL, which were obtained by precipitation of apolipoprotein B-containing lipoproteins. LDL cholesterol levels were calculated. Plasma glucose level was measured by the hexokinase method (Gluco-quant Glucose HK in haemolysate on Roche automated clinical chemistry analysers, Roche Diagnostics). HbA1c level was measured in fasting whole blood samples obtained prior to surgery using the Tina-quant 2nd generation assay on the Cobas Integra 400 plus automated analyser (Roche Diagnostics). ALT and AST were measured by standard procedures using a Dimension Vista system, Flex reagent cartridge (Siemens). Steatohepatitis grading and staging was performed from liver slides stained with haematoxylin and eosin, periodic acid–Schiff–diastase and Masson's trichrome according to the classification proposed by Brunt et al.[39]. All individuals received medications as illustrated in Supplementary Table 1. To mitigate experimental confounders from treatment-mediated traits in microbial profiles[40], individuals were further selected on the basis of diverse medical use.

DNA extraction. DNA was extracted from plasma (200 µl), liver (28–78 mg depending on the sample), MAT (46–103 mg), OAT (28–85 mg) and SAT (45–157 mg) using an optimised blood and tissue-specific technique that was carefully designed to minimise any risk of contamination between samples or from the experimenters. DNA was extracted using a Silica based column after three rounds of mechanical lysis for 30 s at 30 Hz in a bead beater (TissueLyser, Qiagen) with 0.1 mm glass beads (MoBio, Qiagen) to increase the yield of bacterial DNA. Total genomic DNA was collected in 50 µl of molecular grade water. The quality and quantity of extracted DNA were monitored by gel electrophoresis (1% w/w agarose in 0.5× TBE buffer) and NanoDrop 2000 UV spectrophotometer (Thermo Fisher Scientific). All DNA extracts were stored at −20 °C until further processing.

Bacterial quantification by quantitative PCR. Real-time PCR amplification was performed using 16S universal primers that target the V3–V4 region of the bacterial 16S ribosomal gene: primers EUBF 5′-TCCTACGGGAGGCAGCAGT-3′ and EUBR 5′-GGACTACCAGGGTATCTAATCCTGTT-3′. The qPCR step was performed in triplicate on a VIIA 7 PCR system (Life Technologies) using SYBR Green technology and the specificity of all qPCR products was assessed by systematic analysis of a post-PCR dissociation curve performed between 60 °C and 95 °C. The absolute number of copies of the 16S rRNA gene was determined by comparison with a quantitative standard curve generated by serial dilution of plasmid standards. Total 16S rRNA gene count was normalised by mg of tissue or ml of plasma.

16S rRNA gene-based analysis. The V3–V4 hypervariable regions of the 16S rRNA gene (467 bp on the *Escherichia coli* reference genome) were amplified from the DNA extracts during the first PCR step using universal primer Vaiomer 1F (CTTTCCCTACACGACGCTCTTCCGATCT–TCCTACGGGAGGCAGCAGT, partial P5 adapter–primer) and universal primer Vaiomer 1R (GGAGTTCAGACGTGTGCTCTTCCGATCT–GGACTACCAGGGTATCTAATCCTGTT, partial P7 adapter–primer), which are fusion primers based on the qPCR primers. The first PCR reaction was carried out on a Veriti Thermal Cycler (Life Technologies) as follows: an initial denaturation step (94 °C for 10 min), 35 cycles of amplification (94 °C for 1 min, 68 °C for 1 min and 72 °C for 1 min) and a final elongation step at 72 °C for 10 min. Amplicons were then purified using the magnetic beads Agencourt AMPure XP for PCR Purification (Beckman Coulter).

Sample multiplexing was performed using tailor-made 6-bp unique index sequences, which were added during the second PCR step at the same time as the second part of the P5 or P7 adapters used for the sequencing step on the MiSeq flow cells with the forward primer Vaiomer 2F (AATGATACGGCGACCACCGAGATCTACACT–CTTTCCCTACACGAC,

partial P5 adapter–primer targeting primer 1F) and reverse primer Vaiomer 2R (CAAGCAGAAGACGGCATACGAGAT–index–GTGACT–GGAGTTCAGACGTGT, partial P7 adapter including index–primer targeting primer 1R). This second PCR step was performed on 50–200 ng of purified amplicons from the first PCR. The PCR reaction was carried out on a Veriti Thermal Cycler (Life Technologies) and was run as follows: an initial denaturation step (94 °C for 10 min), 12 cycles of amplification (94 °C for 1 min, 65 °C for 1 min and 72 °C for 1 min) and a final elongation step at 72 °C for 10 min. Amplicons were purified as described for the first PCR round. All libraries were pooled in the same quantity in order to generate an equivalent number of raw reads with each library. The detection of the sequencing fragments was performed using MiSeq Illumina technology with 2×300 paired-end MiSeq kit v3. The targeted metagenomic sequences were analysed using a bioinformatics pipeline based on 'find, rapidly, OTUs with Galaxy solution' (FROGS) guidelines[41]. In brief, after demultiplexing of barcoded Illumina paired reads, single read sequences were cleaned and paired into longer fragments for each sample independently. OTUs were produced with single-linkage clustering and taxonomic assignment was performed to determine community profiles. The following filters were applied: first, the last 30 bases of reads R1 and the last 60 bases of reads R2 were removed; second, amplicons with a length of <350 nt or a length of >490 nt were removed and third, OTUs with abundance lower than 0.005% and that appeared less than twice in the entire dataset were removed.

Assessment of potential sample contamination. Samples with low bacterial biomass, such as tissues and plasma, are highly susceptible to potential contamination from environment and reagents[31,32] and therefore to false-positive results. To account for this challenge, we included a comprehensive set of negative controls to test for environmental sample contamination at major steps in the analysis (Fig. 1). In short, during tissue collection, tubes were kept open next to the operation field throughout the entire procedure (air–liver, air–OAT, and air–SAT). Contamination that derived from tissue manipulation was controlled by an additional set of tubes kept open next to the operator throughout blood centrifugation and plasma collection (air–lab) as well as during tissue aliquoting (air–biobank). The cutting board that was used to aliquot tissue samples was sampled prior to tissue manipulation (swab–biobank). Water samples were used to control for labware, reagent and/or environmental contamination during DNA extraction (ext–water) and during amplification steps for tissue 16S rRNA quantification (qPCR–water). After thorough validation of negative controls on a case-by-case basis, 16S rRNA quantification and sequencing data were used for the discovery of tissue-specific bacterial signatures linked to T2D.

Statistical analyses. Participant anthropometric and metabolic features were compared using an unpaired *t*-test or Mann-Whitney *U* test for parametric and non-parametric data sets, respectively, and adjusted for multiple comparisons by the two-stage linear step-up procedure of Benjamini, Krieger and Yekutieli, with $q < 1\%$. Normality was calculated using the Shapiro–Wilk test. For 16S rRNA gene quantification and alpha diversity plots we applied the Kruskal–Wallis one-way analysis of variance (ANOVA) followed by Dunn's test for pairwise comparison and *P* value adjustment using the Bonferroni–Holm method. Permutational multivariate analysis of variance (PERMANOVA), with subsequent Bonferroni–Holm *P* value adjustment, was used to assign statistical significance to the differences between clusters of 16S rRNA sequences that were visualised in PCoA scatterplots. For 16S rRNA sequencing data that compare different tissues of all individuals, we filtered all taxa that were not present in at least 20% of samples within each body site and applied ALDEx2 to extract the taxa that were more likely to constitute tissue-specific bacterial signatures. This method is optimised for sparse and spurious data with multiple zeros, a general characteristic for samples with low bacterial biomass. To validate these findings against negative controls we then performed Kruskal–Wallis tests with Dunn's pairwise comparison and Bonferroni–Holm *P* value adjustment. LEfSe was performed to characterise the tissue-specific taxonomic features that best discriminated patients with diabetes versus individuals with normoglycaemia. In brief, a non-parametric factorial Kruskal–Wallis sum-rank test was first applied to detect taxa with significant differential abundance. Biological significance was subsequently investigated using a set of pairwise tests among subclasses using the unpaired Wilcoxon rank-sum test. As a last step, linear discriminant analysis was used to estimate the effect size of each differentially abundant feature.

Reporting Summary. Further information on research design is available in the Nature Research Reporting Summary linked to this article.

Data availability

Sequencing data was deposited to the European Nucleotide Archive, https://www.ebi.ac.uk/ena, with accession number: PRJEB36477. Secondary accession: ERP119674.

Received: 22 January 2020; Accepted: 5 February 2020;
Published online: 09 March 2020

References

1. Zhang, Y., Niu, J. & Choi, H. K. Excess mortality among persons with type 2 diabetes. *N. Engl. J. Med.* **374**, 788 (2016).
2. Seshasai, S. R., Kaptoge, S., Thompson, A., Di Angelantonio, E. & Gao, P. Diabetes mellitus, fasting glucose, and risk of cause-specific death. *N. Engl. J. Med.* **364**, 829–841 (2011).
3. American Diabetes Association Diagnosis and classification of diabetes mellitus. *Diabetes Care* **37**, S81–S90 (2014).
4. Locke, A. E. et al. Genetic studies of body mass index yield new insights for obesity biology. *Nature* **518**, 197–206 (2015).
5. Ridaura, V. K. et al. Gut microbiota from twins discordant for obesity modulate metabolism in mice. *Science* **341**, 1241214 (2013).
6. Delzenne, N. M., Cani, P. D., Everard, A., Neyrinck, A. M. & Bindels, L. B. Gut microorganisms as promising targets for the management of type 2 diabetes. *Diabetologia* **58**, 2206–2217 (2015).
7. Janesick, A. S., Shioda, T. & Blumberg, B. Transgenerational inheritance of prenatal obesogen exposure. *Mol. Cell. Endocrinol.* **398**, 31–35 (2014).
8. Pedersen, H. K. et al. Human gut microbes impact host serum metabolome and insulin sensitivity. *Nature* **535**, 376–381 (2016).
9. Paisse, S. et al. Comprehensive description of blood microbiome from healthy donors assessed by 16S targeted metagenomic sequencing. *Transfusion* **56**, 1138–1147 (2016).
10. Lluch, J. et al. The characterization of novel tissue microbiota using an optimized 16S metagenomic sequencing pipeline. *PLoS One* **10**, e0142334 (2015).
11. Amar, J. et al. Intestinal mucosal adherence and translocation of commensal bacteria at the early onset of type 2 diabetes: molecular mechanisms and probiotic treatment. *EMBO Mol. Med.* **3**, 559–572 (2011).
12. Lelouvier, B. et al. Changes in blood microbiota profiles associated with liver fibrosis in obese patients: a pilot analysis. *Hepatology* **64**, 2015–2027 (2016).
13. Alvarez-Silva, C. et al. Compartmentalization of immune response and microbial translocation in decompensated cirrhosis. *Front. Immunol.* **10**, 1–11 (2019).
14. Schertzer, J. D. et al. NOD1 activators link innate immunity to insulin resistance. *Diabetes* **60**, 2206–2215 (2011).
15. Cani, P. D. et al. Metabolic endotoxemia initiates obesity and insulin resistance. *Diabetes* **56**, 1761–1772 (2007).
16. Blasco-Baque, V. et al. Periodontitis induced by porphyromonas gingivalis drives periodontal microbiota dysbiosis and insulin resistance via an impaired adaptive immune response. *Gut* **66**, 872–885 (2017).
17. Cavallari, J. F. et al. Muramyl dipeptide-based postbiotics mitigate obesity-induced insulin resistance via IRF4. *Cell Metab.* **25**, 1063–1074.e3 (2017).
18. Denou, E. et al. Defective NOD2 peptidoglycan sensing promotes diet-induced inflammation, dysbiosis, and insulin resistance. *EMBO Mol. Med.* **7**, 259–274 (2015).
19. Verma, R. et al. Cell surface polysaccharides of *Bifidobacterium bifidum* induce the generation of Foxp3$^+$ regulatory T cells. *Sci. Immunol.* **3**, eaat6975 (2018).
20. Schierwagen, R. et al. Trust is good, control is better: technical considerations in blook microbiome analysis. *Gut* https://gut.bmj.com/content/early/2019/06/15/gutjnl-2019-319123 (2019).
21. Schierwagen, R. et al. Circulating microbiome in blood of different circulatory compartments. *Gut* **68**, 578–580 (2019).
22. Le Chatelier, E. et al. Richness of human gut microbiome correlates with metabolic markers. *Nature* **500**, 541–546 (2013).
23. Zeevi, D. et al. Personalized nutrition by prediction of glycemic responses. *Cell* **163**, 1079–1094 (2015).
24. Thingholm, L. B. et al. Obese individuals with and without type 2 diabetes show different gut microbial functional capacity and composition. *Cell Host Microbe* **26**, 252–264.e10 (2019).
25. Sokol, H. et al. *Faecalibacterium prausnitzii* is an anti-inflammatory commensal bacterium identified by gut microbiota analysis of Crohn disease patients. *Proc. Natl Acad. Sci. USA* **105**, 16731–16736 (2008).
26. Salomäki-Myftari, H. et al. Neuropeptide Y overexpressing female and male mice show divergent metabolic but not gut microbial responses to prenatal metformin exposure. *PLoS One* **11**, e0163805 (2016).
27. Verdam, F. J. et al. Human intestinal microbiota composition is associated with local and systemic inflammation in obesity. *Obesity (Silver Spring).* **21**, E607–E615 (2013).
28. Natividad, J. M. et al. *Bilophila wadsworthia* aggravates high fat diet induced metabolic dysfunctions in mice. *Nat. Commun.* **9**, 2802 (2018).
29. Jensen, B. A. H. et al. Lysates of *Methylococcus capsulatus* Bath induce a lean-like microbiota, intestinal FoxP3$^+$RORγt$^+$IL-17$^+$ Tregs and improve metabolism. Preprint at *bioRxiv* https://doi.org/10.1101/855486 (2019).
30. de Goffau, M. C. et al. Human placenta has no microbiome but can contain potential pathogens. *Nature* **572**, 329–334 (2019).
31. Salter, S. J. et al. Reagent and laboratory contamination can critically impact sequence-based microbiome analyses. *BMC Biol.* **12**, 1–12 (2014).

32. Glassing, A., Dowd, S. E., Galandiuk, S., Davis, B. & Chiodini, R. J. Inherent bacterial DNA contamination of extraction and sequencing reagents may affect interpretation of microbiota in low bacterial biomass samples. *Gut Pathog.* **8**, 1–12 (2016).
33. Mowat, A. M. & Agace, W. W. Regional specialization within the intestinal immune system. *Nat. Rev. Immunol.* **14**, 667–685 (2014).
34. Thaiss, C. A. et al. Hyperglycemia drives intestinal barrier dysfunction and risk for enteric infection. *Science* **359**, 1376–1383 (2018).
35. Park, C. et al. Obesity modulates intestinal intraepithelial T cell persistence, CD103 and CCR9 expression, and outcome in dextran sulfate sodium–induced Colitis. *J. Immunol.* **203**, 3427–3435 (2019).
36. Petersen, C. et al. T cell-mediated regulation of the microbiota protects against obesity. *Science* **365**, eaat9351 (2019).
37. Luck, H. et al. Gut-associated IgA^+ immune cells regulate obesity-related insulin resistance. *Nat. Commun.* **10**, 3650 (2019).
38. Castillo, D. J., Rifkin, R. F., Cowan, D. A. & Potgieter, M. The healthy human blood microbiome: fact or fiction?. *Front. Cell. Infect. Microbiol.* **9**, 148 (2019).
39. Brunt, E. M., Janney, C. G., Di Bisceglie, A. M., Neuschwander-Tetri, B. A. & Bacon, B. R. Nonalcoholic steatohepatitis: a proposal for grading and staging the histological lesions. *Am. J. Gastroenterol.* **94**, 2467–2474 (1999).
40. Forslund, K. et al. Disentangling type 2 diabetes and metformin treatment signatures in the human gut microbiota. *Nature* **528**, 262–266 (2015).
41. Escudie, F. et al. FROGS: find, rapidly, OTUs with Galaxy solution. *Bioinformatics* **34**, 1287–1294 (2018).

Acknowledgements

This study was supported by a bariatric care team grant (TB2-138776) and a Canadian Microbiome Initiative team grant (MRT-168045) from the Canadian Institutes of Health Research (CIHR) and by a CIHR Foundation Scheme grant to A.M. (FDN-143247). A.M. was supported by a CIHR and Pfizer research chair in the pathogenesis of insulin resistance and cardiovascular diseases. F.F.A. holds a CIHR postdoctoral fellowship and Diabetes Canada incentive funding. B.A.H.J. was supported by awards from the Lundbeck Foundation (R232-2016-2425) and Novo Nordisk Foundation (NNF17OC0026698).

Author contributions

A.M., A.T., F.F.A. and B.A.H.J. conceived and planned the study. A.T., B.A.H.J. and F.F.A. identified and selected the patient cohort. S.M. and L.B. conducted tissue biopsies. B.L. led tissue 16S rRNA gene quantification and sequencing. F.S., S.V.B. and T.V.V. carried out bioinformatic analysis. F.F.A. and T.V.V. generated the figures. F.F.A. and B.A.H.J. integrated the data and wrote the manuscript. F.F.A, B.A.H.J., T.V.V., F.S., S.V.B., D.R., S.M., M.S., L.B., B.L., J.D.S., A.T. and A.M. contributed to data analysis and discussion and agreed upon the submitted manuscript.

Competing interests

The authors declare no competing interests.

Additional information

Extended data is available for this paper at https://doi.org/10.1038/s42255-020-0178-9.

Supplementary information is available for this paper at https://doi.org/10.1038/s42255-020-0178-9.

Correspondence and requests for materials should be addressed to A.M.

Peer review information Primary Handling Editors: Christoph Schmitt; Pooja Jha.

Reprints and permissions information is available at www.nature.com/reprints.

Publisher's note Springer Nature remains neutral with regard to jurisdictional claims in published maps and institutional affiliations.

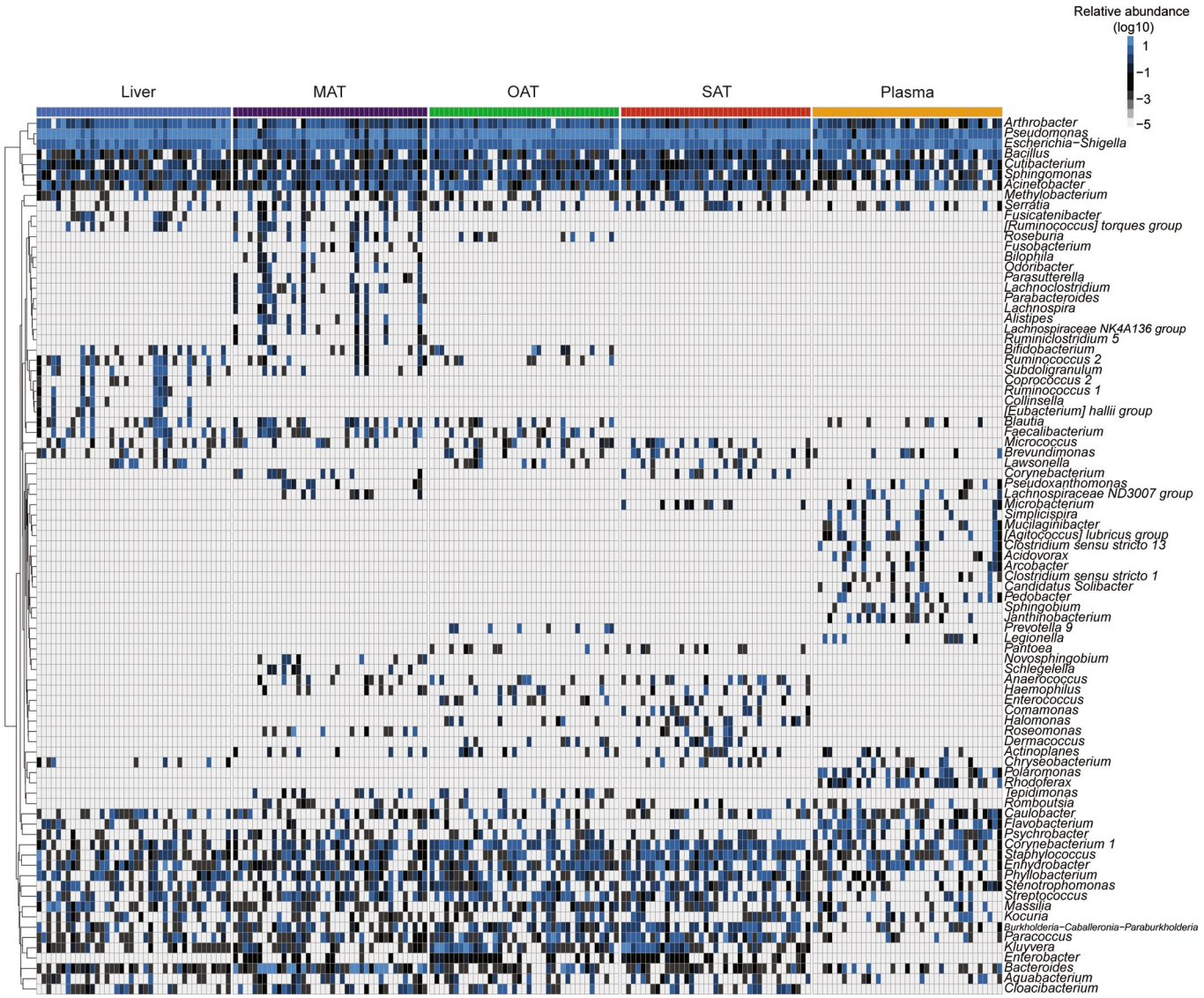

Extended Data Fig. 1 | Genera distribution in the liver, plasma and mesenteric, omental and subcutaneous adipose tissue of obese subjects. Filtered genera were plotted in a heatmap whereby genus abundance is depicted for each sample within each tissue analyzed. Dendograms on the left of heatmaps are based on correlations of abundance profile.

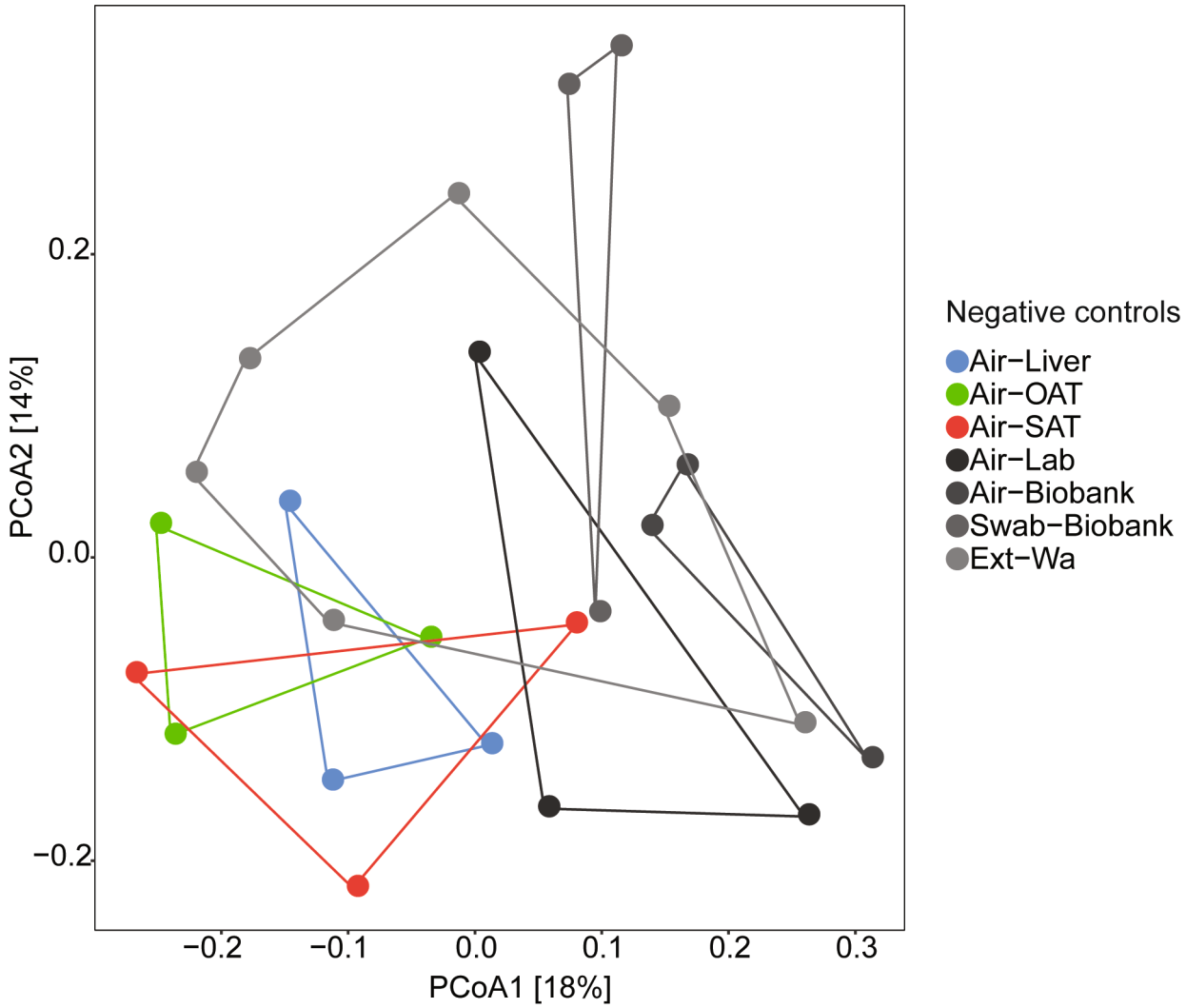

	Adj. P value	R^2	Df	F
Air-Liver vs Air-OAT	1.0	0.14	5	0.69
Air-Liver vs Air-SAT	0.9	0.14	5	0.69
Air-Liver vs Air-Lab	0.4	0.21	5	1.11
Air-Liver vs Air-Biobank	0.2	0.27	5	1.53
Air-Liver vs Swab-Biobank	0.2	0.30	5	1.73
Air-Liver vs Ext-Wa	0.7	0.09	8	0.71
Air-OAT vs Air-SAT	1.0	0.12	5	0.59
Air-OAT vs Air-Lab	0.3	0.35	5	2.21
Air-OAT vs Air-Biobank	0.1	0.35	5	2.21
Air-OAT vs Swab-Biobank	0.1	0.36	5	2.27
Air-OAT vs Ext-Wa	0.2	0.14	8	1.17
Air-SAT vs Air-Lab	0.2	0.28	5	1.60
Air-SAT vs Swab-Biobank	0.2	0.32	5	1.91
Air-SAT vs Ext-Wa	0.4	0.12	8	1.03
Air-Lab vs Air-Biobank	0.9	0.14	5	0.68
Air-Lab vs Swab-Biobank	0.2	0.25	5	1.37
Air-Biobank vs Swab-Biobank	0.2	0.14	8	1.22
Air-Biobank vs Ext-Wa	0.2	0.26	5	1.41
Swab-Biobank vs Ext-Wa	0.3	0.14	8	1.15

Extended Data Fig. 2 | Principal Coordinate Analysis on generalized UniFrac distances of 16S sequences from negative controls. Permutational multivariate analysis of variance (PERMANOVA), with subsequent Bonferroni-Holm P adjustment, was used to assign statistical significance to the differences between clusters of 16S sequences. The number of independent biological samples tested was: Air-Liver (n=3), Air-OAT (n=2), Air-SAT (n=3). The number of technical replicates tested was: Air-Lab (n=3), Air-Biobank (n=3), Swab-Biobank (n=3), Ext-Wa (n=6). Each dot represents a sample. All statistical testes were two-sided, and differences were considered statistically significant at $P<0.05$.

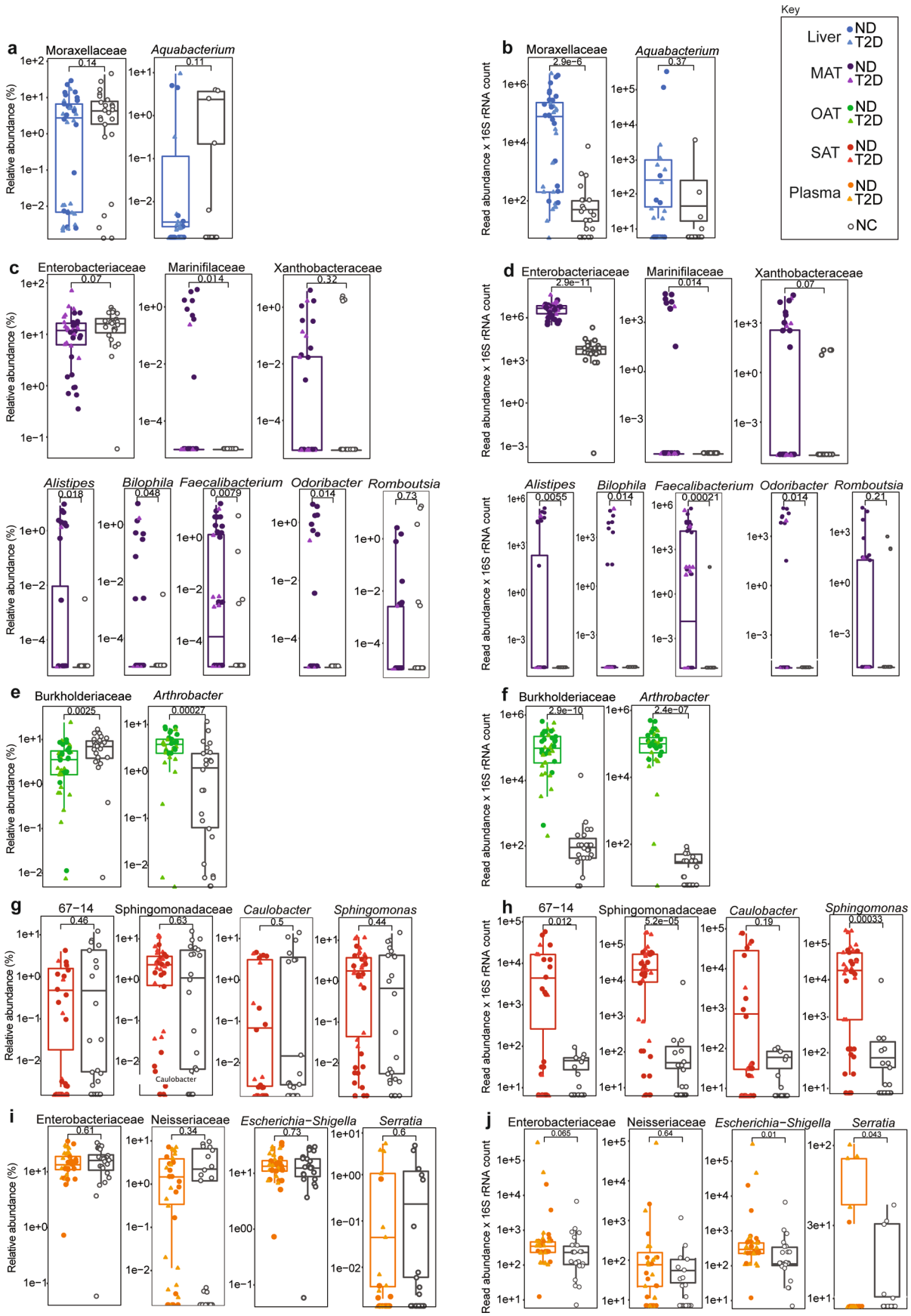

Extended Data Fig. 3 | see figure caption on next page.

Extended Data Fig. 3 | Validation with negative controls of tissue-specific taxa different between participants who were normoglycemic or type 2 diabetic. Tissue-specific bacterial targets found to discriminate between disease state were identified by LefSe analysis. The relative abundance of these taxa (at family and genus level) in liver (**a, b**), mesenteric (MAT – **c, d**), omental (OAT – **e, f**) and subcutaneous (SAT – **g, h**) adipose tissue and plasma (**i, j**) was analyzed, without accounting for disease state distribution, against negative controls (NCs) using Mann-Whitney U test. P values are indicated at the top of each graph. Left side panels show the relative abundance of taxa, whereas right side panels depict relative abundance normalized by 16S rRNA gene count (that is, relative abundance x 16S count). Box plots depict the first and the third quartile with the median represented by a vertical line within the box; the whiskers extend from the first and third quartiles to the highest and lowest observation, respectively, not exceeding 1.5 x IQR. Each circle (Non-diabetic, ND) and triangle (Type 2 Diabetic, T2D) represents a sample, and their tissue-specific dispersion is presented using a log10 scale. The number of independent biological replicates tested was: Liver (n=39), MAT (n=40), OAT (n=40), SAT (n=40), Plasma (n=39), NC (n=23). All statistical tests were two-sided, and differences were considered statistically significant at $P<0.05$.

nature research

Corresponding author(s): NATMETAB-A20012251-T

Last updated by author(s): Jan 30, 2020

Reporting Summary

Nature Research wishes to improve the reproducibility of the work that we publish. This form provides structure for consistency and transparency in reporting. For further information on Nature Research policies, see Authors & Referees and the Editorial Policy Checklist.

Statistics

For all statistical analyses, confirm that the following items are present in the figure legend, table legend, main text, or Methods section.

n/a	Confirmed
☐	☒ The exact sample size (*n*) for each experimental group/condition, given as a discrete number and unit of measurement
☐	☒ A statement on whether measurements were taken from distinct samples or whether the same sample was measured repeatedly
☐	☒ The statistical test(s) used AND whether they are one- or two-sided *Only common tests should be described solely by name; describe more complex techniques in the Methods section.*
☐	☒ A description of all covariates tested
☐	☒ A description of any assumptions or corrections, such as tests of normality and adjustment for multiple comparisons
☐	☒ A full description of the statistical parameters including central tendency (e.g. means) or other basic estimates (e.g. regression coefficient) AND variation (e.g. standard deviation) or associated estimates of uncertainty (e.g. confidence intervals)
☐	☒ For null hypothesis testing, the test statistic (e.g. *F*, *t*, *r*) with confidence intervals, effect sizes, degrees of freedom and *P* value noted *Give P values as exact values whenever suitable.*
☒	☐ For Bayesian analysis, information on the choice of priors and Markov chain Monte Carlo settings
☒	☐ For hierarchical and complex designs, identification of the appropriate level for tests and full reporting of outcomes
☐	☒ Estimates of effect sizes (e.g. Cohen's *d*, Pearson's *r*), indicating how they were calculated

Our web collection on statistics for biologists contains articles on many of the points above.

Software and code

Policy information about availability of computer code

Data collection	Sequencing data were collected using the NG6 open source environment (https://www.ncbi.nlm.nih.gov/pubmed/22958229) version 2.0. Detailed bioinformatics pipeline is described in the manuscript (material and methods section). We used FROGS v1.4.0 for OTU picking from 16S sequences and Blast+ v2.2.30+ with the databank Silva 128 Parc for taxonomic assignement. PhyloSeq v1.14.0 package for R package was used to import, storage, analysis, and graphical display of microbiome census data.
Data analysis	PhyloSeq v1.14.0 package for R.

For manuscripts utilizing custom algorithms or software that are central to the research but not yet described in published literature, software must be made available to editors/reviewers. We strongly encourage code deposition in a community repository (e.g. GitHub). See the Nature Research guidelines for submitting code & software for further information.

Data

Policy information about availability of data

All manuscripts must include a data availability statement. This statement should provide the following information, where applicable:

- Accession codes, unique identifiers, or web links for publicly available datasets
- A list of figures that have associated raw data
- A description of any restrictions on data availability

The datasets and codes generated during and/or analysed during the current study are available from the corresponding author on reasonable request. Sequence data has been deposited at the European Nucleotide database, https://www.ebi.ac.uk/ena, with accession number: PRJEB36477, secondary accession: ERP119674.

Field-specific reporting

Please select the one below that is the best fit for your research. If you are not sure, read the appropriate sections before making your selection.

☒ Life sciences ☐ Behavioural & social sciences ☐ Ecological, evolutionary & environmental sciences

For a reference copy of the document with all sections, see nature.com/documents/nr-reporting-summary-flat.pdf

Life sciences study design

All studies must disclose on these points even when the disclosure is negative.

Sample size	No sample size pre-calculation was performed. We applied rigorous non-parametric statistical tests and corrected for multiple comparisons (where applicable) to ensure that detected differences in this study were not observed by chance and that sample size was enough to rule out randomness.
Data exclusions	We took careful measures to ensure that the contamination-aware strategy adopted in this study would not be skewed by contamination during tissue preparation and DNA extraction/amplification/sequencing not accounted for in our negative controls. Whenever this happened (or if there was at least a risk), we conducted careful analysis by observational criteria during data analysis to confirm that the sample was indeed compromised. We therefore withdraw from our16S sequencing data one sample from the group SAT and one from OAT. We excluded from the 16S rRNA quantification data one sample from the group LIVER due to technical reasons.
Replication	We applied rigorous non-parametric statistical tests and corrected for multiple comparisons (where applicable) to ensure that detected differences in this study were not observed by chance, but rather constitute a reliable measure with high level of reproducibility.
Randomization	Patients were allocated to groups according to their fasting blood glucose (FBG) and glycated hemoglobin (HbA1c) levels (Normoglycemic: HbA1c below 5.7 % or FBG below 6.1 mM; type 2 diabetes: FBG above 7.0 mM or HbA1c greater than 6.5 %). Covariates were controlled using unpaired t-test for parametric data sets or Mann-Whitney U-test for non-parametric data sets. Normality was calculated using Shapiro-Wilk test.
Blinding	Investigators were blinded during data collection and analysis.

Reporting for specific materials, systems and methods

We require information from authors about some types of materials, experimental systems and methods used in many studies. Here, indicate whether each material, system or method listed is relevant to your study. If you are not sure if a list item applies to your research, read the appropriate section before selecting a response.

Materials & experimental systems

n/a	Involved in the study
☒	☐ Antibodies
☒	☐ Eukaryotic cell lines
☒	☐ Palaeontology
☒	☐ Animals and other organisms
☐	☒ Human research participants
☐	☒ Clinical data

Methods

n/a	Involved in the study
☒	☐ ChIP-seq
☒	☐ Flow cytometry
☒	☐ MRI-based neuroimaging

Human research participants

Policy information about studies involving human research participants

Population characteristics	The cohort included 10 men and 30 women, which reflects the proportion of each sex in the IUCPQ bariatric practice. A total of n=20 participants (5 men, 15 women) had normal glucose tolerance described by a HbA1c below 5.7 % or fasting plasma glucose below 6.1 mM, whereas n=20 participants (5 men, 15 women) had type 2 diabetes, with fasting plasma glucose above 7.0 mM or HbA1c ≥ 6.5 %
Recruitment	Tissue samples were obtained from the Biobank of the Institut universitaire de cardiologie et de pneumologie de Québec - Université Laval (IUCPQ) according to institutionally-approved management modalities. All participants provided written, informed consent.
Ethics oversight	Ethical approval was granted by Canadian Institute of Health and Research, #2017-2746 21386. All participants provided written informed consent and the study complied with the parameters established by the Laval University Ethics Board.

Note that full information on the approval of the study protocol must also be provided in the manuscript.

Clinical data

Policy information about clinical studies

All manuscripts should comply with the ICMJE guidelines for publication of clinical research and a completed CONSORT checklist must be included with all submissions.

Clinical trial registration	This study is not a clinical trial
Study protocol	na
Data collection	na
Outcomes	na